

PAPER • OPEN ACCESS

The Single Deposit Scale Scenario at Granite Area in A Long-Term Safety Assessment of A Radioactive Waste Repository

To cite this article: Jiebiao Li *et al* 2019 *IOP Conf. Ser.: Earth Environ. Sci.* **237** 022012

View the [article online](#) for updates and enhancements.



IOP | ebooks™

Bringing you innovative digital publishing with leading voices to create your essential collection of books in STEM research.

Start exploring the collection - download the first chapter of every title for free.

The Single Deposit Scale Scenario at Granite Area in A Long-Term Safety Assessment of A Radioactive Waste Repository

Jiebiao Li, Rui Su, Zhichao Zhou*

CNNC Key Laboratory on Geological Disposal of High-level Radioactive Waste, Beijing Research Institute of Uranium Geology, Beijing 100029, China

*Corresponding author's e-mail: zhouzhichao2006@163.com

Abstract. Deep geological disposal is internationally accepted as a feasible and safe way to dispose of high-level radioactive waste (HLW). Long-term safety assessment of a radioactive waste repository is vital to building confidence in safety of geological disposal of radioactive waste. Many countries with nuclear power industries have carried out this work. The aim of this paper is to study the influence by a fracture intersecting the deposition hole or excavation damaged zone at repository located in granite area. Furthermore, it is also of interest for addressing important aspects of the internal evolution of the canister. This paper analysed two representative scenarios for the single deposit scale scenario at granite area. These results show that the influence of the fracture zone is enormous. The convective transport mass is far more than the diffusive transport mass. Moreover, the leading path of convective is the fracture zone. The transport mass which across the granite boundary is very little. These results also a convenient case for the construction of final geological repositories in China.

1. Introduction

Safe disposal of HLW is a challenging task for the sustainable development of nuclear energy and environmental protection [Witherspoon 2001; Wang et al.2018]. Deep geological waste repositories are designed to ensure safety from radiation for thousands of years and many countries have considered building deep geological repositories. [IAEA&NEA, 2006; Ales' et al.2015]. Long-term safety assessment is one of the most important phases for geological repositories of HLW. In additional, the long-term safety assessment has been widely studied to improve the confidence in the safety of the system. [Campbell and Cranwell, 1988].

From the point of view of a long-term safety assessment, various scenarios related to the release and migration of radionuclides can be occurred [SKB 2006; DOE 2008; SKB 2011; Kim et al.2014]. The purpose of the safety assessment project includes making a first assessment of the safety of potential repositories to dispose of canisters, to provide feedback to design development and to foster a dialogue with the authorities that oversee activities.

In 2011, SKB had published their final safety assessment report of the SR-Site project to support SKB's license application for a final repository at Forsmark site in Sweden [SKB, 2011]. In 2012, POSIVA completed and submitted the safety assessment report about Olkiluoto site in Finland [PosivaOy, 2012]. At present, China has carried out some initial studies on long-term safety assessment through international cooperation, and basic capabilities of safety assessment have been acquired, but key technologies have not been fully mastered [Ling, 2018].



The objective of this study is to understand the influence by a fracture intersecting the deposition hole or excavation damaged zone at repository located in granite area. Furthermore, it is also of interest for addressing important aspects of the internal evolution of the canister.

In this work, two representative scenarios are analyzed. For China, the currently pursuing site is located at granite area [Wang, 2010]. It is, therefore, also a convenient case for demonstrating the damage of these potential failure modes. It is vital to making clear the internal evolution of the canister.

2. Introduce and background

In the final repository, radionuclides maybe leaking out through a small hole in the canister wall diffuse into the buffer and may then migrate through various pathways into the flowing water in rock fractures. These nuclides escape from a copper/iron canister through a small hole into the bentonite by diffusion. In the interior of bentonite, they migrate through various pathways into the water flowing in the rock. There maybe three-radionuclide release path that from the canister into the biosphere [SKB, 2009]. These are the Q1 path, with transport in a fracture intersecting the deposition hole; the Q2 path, with transport in the excavation-damaged zone (EDZ); and the Q3 path, with transport in the deposition tunnel to an intersecting fracture.

To solve this problem, two scenarios were set up. Scenario 1(modelling 1) only considered the path Q2 and scenario 2(modelling 2) considered both path Q1 and path Q2. To simply the model, the path Q3 ignored in this work. In addition, the canister assumed as an integral. Moreover, the fuel release with a constant rate, i.e. the concentration of the canister was set to be 1unit from 1000 to 10000 years. Both the two safety cases were set as a steady state problem.

3. Scenario 1 in the single deposit scale at granite area

3.1 Modelling 1 description

In this case, the range of the modelling is 6 x 40 x 23.3 m, in which consisting of a low permeability porous medium (granite), one canister (do not consider the component of the canister), one tunnel.

Referring to the SR-Can project report [SKB, 2009], the specific geometric data for the modelling 1 used as follows,

The tunnel spacing fixed at 40m, and length and width both are 5.5m.

The distance between canister centers is 6m.

The copper shell is 50 mm thick and the cylindrical canister has a length of approximately 4.8 m and a diameter of 1.05 m.

The deposition hole has a length of approximately 7.8m and a diameter of 1.75m.

The distance between canister bottom and the deposition hole bottom is 0.5m.

The depth of the excavation damaged zone about 1.0m.

The size of the fracture aperture is 1000mm.

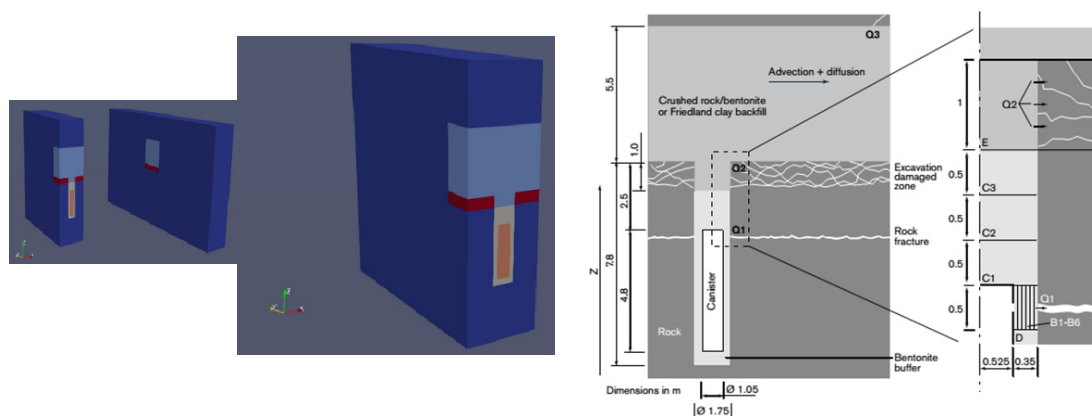


Figure 1. The layout of modelling 1

For the pressure boundary: The bottom of the model has constant pressure and horizontal gradient, the formula is $298 + 0.003X$. The top of the model also has constant pressure and horizontal gradient, the formula is $298 + 0.003X$. The left of the boundary has the constant pressure, the value of 298. The right of the boundary has the constant pressure, the value of 298.018. The boundary in Y+ and Y- direction are both set to be no-flow boundary.

For the RN concentration boundary: The top and bottom boundary are both set to be constant boundary, the value is both zero. The boundary in X+ and X- directions except the EDZ zone are both set to be no-flux boundary. The EDZ zone boundary in X+ direction set to be constant boundary, the value is 0.0. The EDZ zone boundary in X- direction set to be no-gradient boundary. The boundary in Y+ and Y- direction are both set to be no-flux boundary.

The hydraulic properties see the Table 1. In addition, the buffer defect zone caused by the canister defect, this value only used in the scenario 2. The half-life of the radionuclides is $1.57E+07$ years, and the initial concentration of radionuclide value is 1 unit.

Table 1. Hydraulic properties for Modelling

Subdomain	Porosity	Hydraulic conductivity in three direction (m/yr)			Compressibility	Retardation coefficient	Effective diffusivity (m^2/yr)
		X	Y	Z			
Granite	0.005	3.15E-4	3.15E-4	3.15E-4	1.0E-10	1.00	1.31E-04
Backfill	0.14	3.15E-5	3.15E-5	3.15E-5	1.0E-10	1.00	1.32E-03
Buffer	0.17	3.15E-5	3.15E-5	3.15E-5	1.0E-10	1.00	3.15E-04
Canister	0.20	10	10	10	1.0E-10	1.00	0.063
EDZ	0.10	0.315	0.315	0.315	1.0E-10	1.00	1.31E-02
Buffer defect zone	0.20	3.15E-4	3.15E-4	3.15E-4	1.0E-10	1.00	3.15E-03
Fracture	0.10	9.46	9.46	9.46	1.0E-10	1.00	1.31E-02

3.2 Simulation results of modelling 1

Figure 2 shows the results of spatial distribution of radionuclide concentration at 1000 years, 10000 years, 100,000 years, and 100,000 years after the repository closed. Figures 3 to 5 show the results of the radionuclide transport with time for different subdomains. Table 2 shows the total radionuclide transport at different boundaries of different subdomains.

For the total-domain, the total flux out mass in Z+ direction is about 1/8 in Z- direction. It also can be observed that convective transport mass is bigger than the diffusive transport mass, which is about 3 times.

For the EDZ zone, there is only diffusive happen in the X+ direction boundary. The transport value is about 2/9 of the total outflow flux. Otherwise, there is only convective happen in the X- direction boundary. The value is about 2/3 of the total outflow flux. The biggest value occurred at about 13400 years after the repository closed.

For the canister zone, it is clearly seen that the spatial distribution of concentration nearly symmetry except the Z direction. Most of the radionuclides will flux out through Z+ direction. In additional, the convective transport mode can be negligible in the Y and the Z directions. It should be noted that there is convective mode happened in the X direction.

To summarize, the transport mode of each subdomain is described as follows (see the Figure 6):

Because of the low permeability of the granite, the total convective mass should nearly zero.

For the canister, the convective mode exits the zone can be negligible in the Y and the Z directions. In additional, in the X direction the value is also very small.

For the deposit zone (the extent is same as the deposit hole), the main transport mode is diffusion. The total diffusion mass in the Z direction is smaller than other directions, especially in the Z- direction. The main exit boundary through convective mode is X- and X+ direction boundaries. Compared with the diffusion mass, the value still very small.

In a word, the most expected release path where from the canister enter the buffer zone, and then diffusion into the EDZ zone, finally exits from the X- direction boundary by convective mode, actually the transport mass is very big. These results indicate that the EDZ zone has significant influence for the transport.

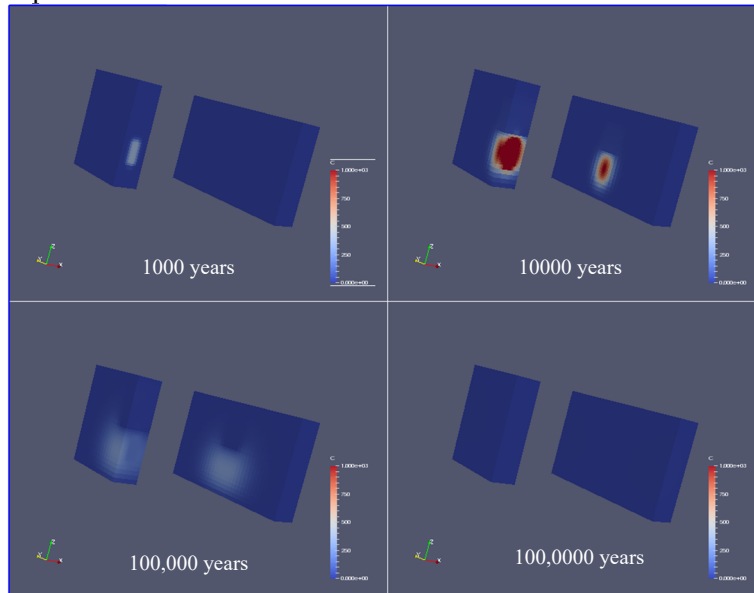


Figure 2. The spatial distribution of radionuclide ‘C’ concentration at 1000 years, 10000 years, 100,000 years, and 100,000 years after the repository closed

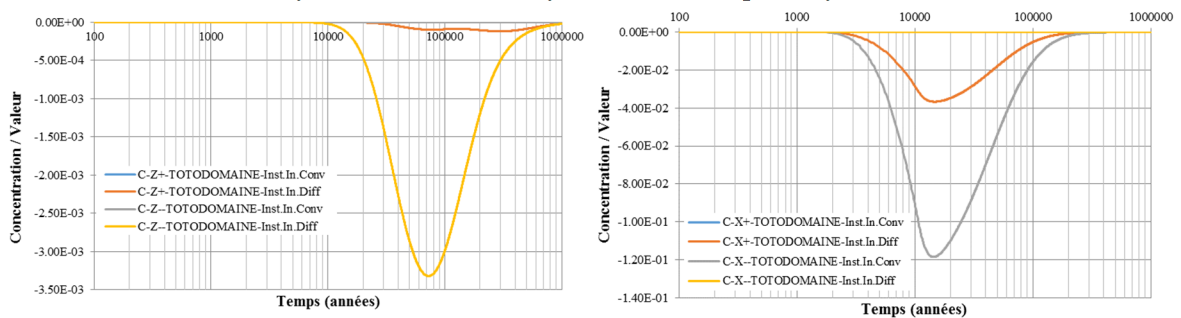


Figure 3. Result of the radionuclide transport with time in different directions for the total domain

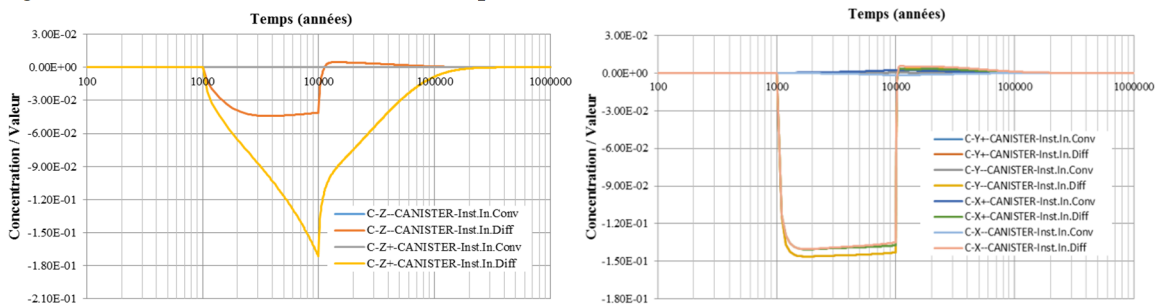


Figure 4. Result of the radionuclide transport with time in different directions for canister

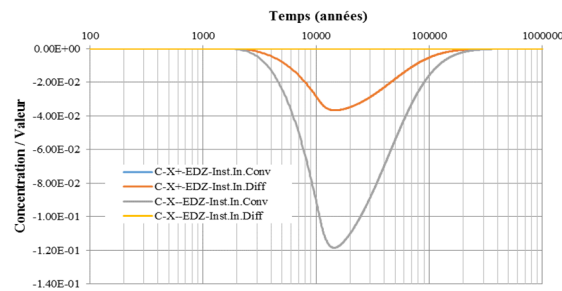


Figure 5. Result of the radionuclide transport with time in different directions for the EDZ domain

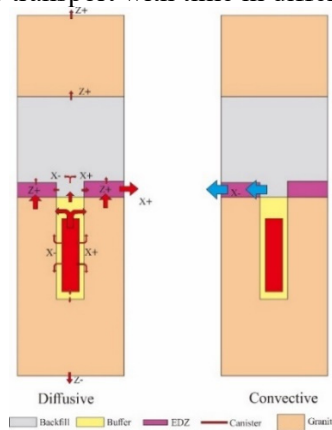


Figure 6. The transport mode of modelling 1

Table 2. The total radionuclide transport at different boundaries of different domains

Boundary	Convective	Diffusive	Total
EDZ in X+ direction	0	-2026.894	-2026.894
EDZ in X- direction	-6218.363	0	-6218.363
DEPOSIT in X+ direction	123.797	-2240.168	-2116.371
DEPOSIT in X- direction	-109.915	-1660.310	-1770.225
DEPOSIT in Y+ direction	7.142	-1928.140	-1920.998
DEPOSIT in Y- direction	7.187	-1928.105	-1920.918
DEPOSIT in Z+ direction	0.016	-1060.277	-1060.261
DEPOSIT in Z- direction	1.482	-138.587	-137.105
Canister in X+ direction	88.158	-1076.008	-987.850
Canister in X- direction	-73.693	-918.272	-991.965
Canister in Y+ direction	7.688	-1074.107	-1066.419
Canister in Y- direction	7.722	-1074.081	-1066.359
Canister in Z+ direction	2.635	-4699.549	-4696.914
Canister in Z- direction	1.783	-140.785	-139.002
TOTDOMAINE in X+ direction	0	-2026.894	-2026.894
TOTDOMAINE in X- direction	-6218.363	0	-6218.363
TOTDOMAINE in Z+ direction	0	-69.298	-69.298
Canister in X+ direction	0	-577.063	-577.063

4. Scenario 2 in the single deposit scale at granite area

4.1 Modelling 2 description

In this case, a horizontal fracture was considered. In addition, a buffer defect zone was also considered which may be caused by the canister defect (the value was listed in the Table 1), the size assumed same with the fracture. By this case, it is easy to understand the sensitivity of the fracture zone. In this case, the size of the fracture aperture is 1000 mm. The other conditions are same with scenario 1.

For the pressure boundary: The bottom of the model has constant pressure and horizontal gradient, the formula is $298 + 0.003X$. The top of the model also has constant pressure and horizontal gradient, the formula is $298 + 0.003X$. The left of the boundary set the constant pressure, the value is 298. The right of the boundary set the constant pressure, the value is 298.018. The boundary in Y+ and Y- direction are both set to be no-flow boundary.

For the RN concentration boundary: The top and bottom boundary are both set to be constant boundary, the value is both zero. The boundary in X+ and X- directions except the EDZ zone and the fracture zone are both set to be no-flux boundary. The EDZ zone boundary in X+ direction set to be constant boundary, the value is 0.0. The EDZ zone boundary in X- direction set to be no-gradient boundary. The fracture zone boundary in X+ direction set to be constant boundary, the value is 0.0. The fracture zone boundary in X- direction set to be no-gradient boundary.

The boundary in Y+ and Y- direction are both set to be no-flux boundary. This case also was set as a steady state problem.

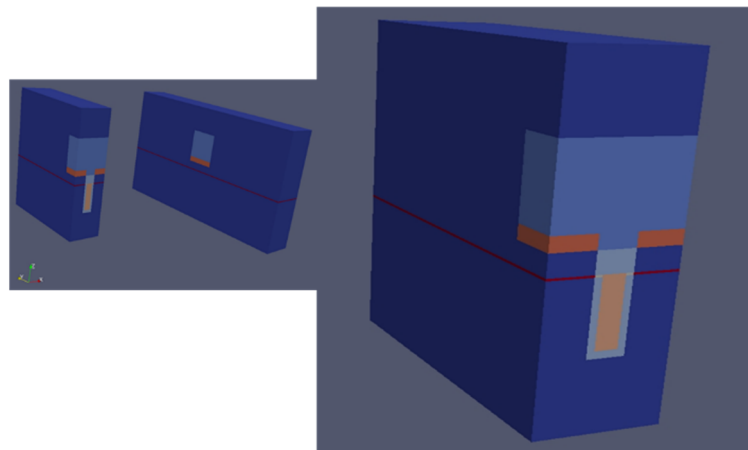


Figure 7. The layout of modelling 2

4.2 Simulation results of modelling 2

Figure 8 shows the results of spatial distribution of radionuclide concentration at 1000 years, 9000 years, 10,000 years, and 100,000 years after the repository closed. Figures 9 to 12 show the results of the radionuclide transport with time for different subdomains. Table 3 shows the total radionuclide transport at different boundaries of different subdomains. It's clearly seen that the results have big different with modelling 1. In this case, most of the radionuclides will flux out through fracture zone.

For the total-domain, the convective transport mass is far more than the diffusive transport mass, which more than 55 times. The total convective transport mass which across the fracture zone is about 81 times of the EDZ zone. Therefore, the leading path of convective is the fracture zone. The main exit boundary of the diffusive happen in the Z- direction boundary. The diffusive mass crosses the Z+ direction boundary is negligible. The total diffusive mass crosses the X+ boundary is also negligible. In additional, the peak concentration happened about at 10000 years after the repository closed. This is almost consistent with the end time of spent fuel release.

For the EDZ zone, only convection transport mode crosses the X+ direction boundary, the value is negligible. Otherwise, only diffusion transport mode crosses the X- direction boundary, the value is also small.

For the fracture, it is clearly that the total convective mass is very large. The total convective mass crosses the fracture boundary in the X- direction is about 97.5% of the source influx. However, the total convective mass crosses the EDZ boundary in the X- direction is about 1.2% of the source influx.

For the canister zone, the main transport mode is also convective transport mode. The total convective mass is about 70% of the source influx crosses the X- direction boundary. It's also can be observed that the convective mass will flux into the region through X+ direction boundary. The diffusion transport main happens in the X+ and Y direction.

For the deposit zone, the dominate mode is also convective. The diffusion transport mass is far less than the convective mass.

To summarize, the transport mode of each subdomain is described as follows (see the Figure 13):

Because of the low permeability of the granite, the total convective mass should nearly zero.

For the canister zone, the main transport mode is convective transport mode. The main exit boundary is X- boundary. It's also can be observed that the convective mass will flux into the region through X+ direction boundary. The diffusion mode exits the zone is very small in the Z and the X- directions. In the other directions is nearly same.

For the deposit zone (the extent is same as the deposit hole), the main transport mode is convective. Most of the radionuclides flux out via the buffer defect zone. The diffusion transport mass crosses the buffer defect zone is negligible.

For the total-domain, the convective transport mass is far more than the diffusive transport mass. The exit boundary of the convective only happen in the X- direction boundary. The main exit boundary of the diffusive happen in the Z- direction boundary. The diffusive mass crosses the Z+ and X+ direction boundary is very small.

In a word, the most expected transport path where from the canister enter the buffer defect zone, and then enter the fracture zone, finally convective out from the fracture (The direction is the same as that of hydraulic gradient). Moreover, the transport mass is very large. These results indicate that the fracture zone has magnificent influence for the transport.

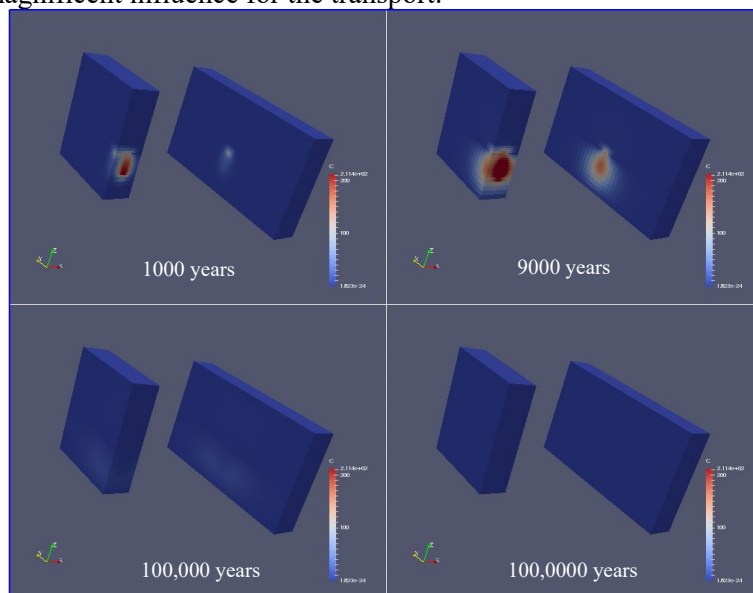


Figure 8. The spatial distribution of radionuclide 'C' concentration at 1000 years, 9000 years, 10, 000 years, and 100, 000 years after the repository closed

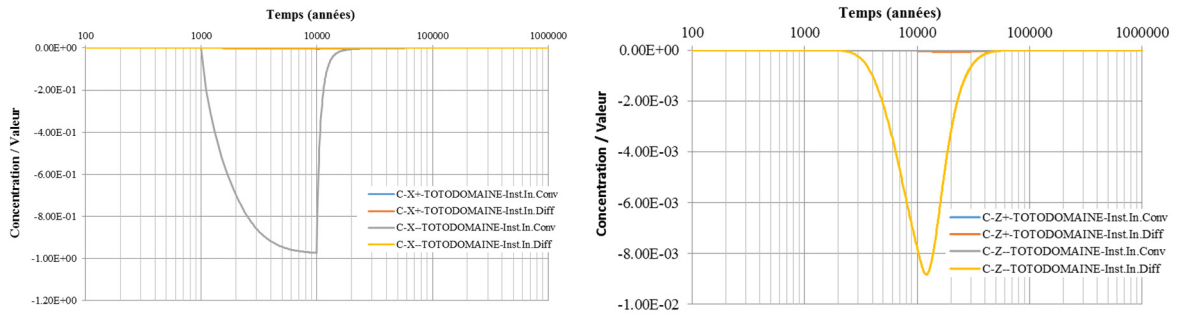


Figure 9. Result of the radionuclide transport with time in different directions for the total domain

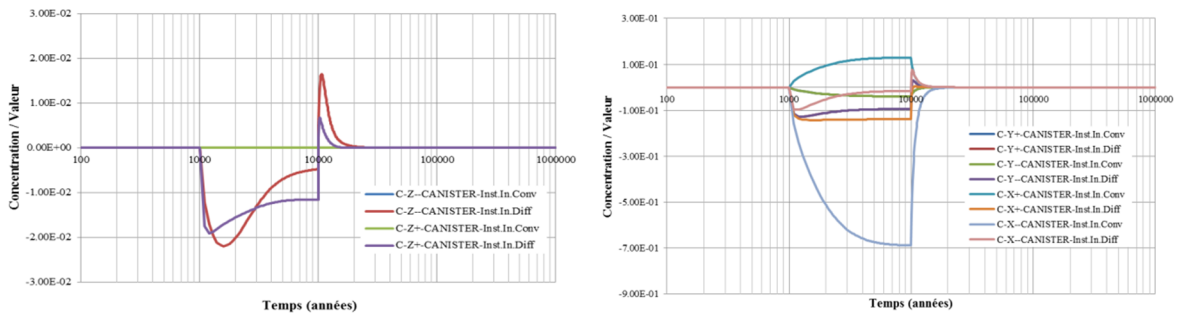


Figure 10. Result of the radionuclide transport with time in different directions for the canister

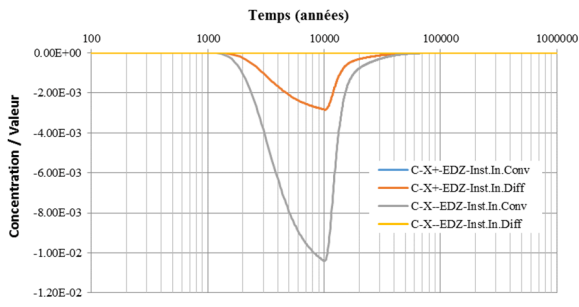


Figure 11. Result of the radionuclide transport with time in different directions for the EDZ zone

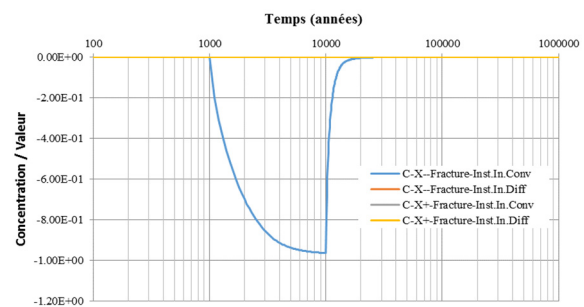


Figure 12. Result of the radionuclide transport with time in different directions for the fracture zone

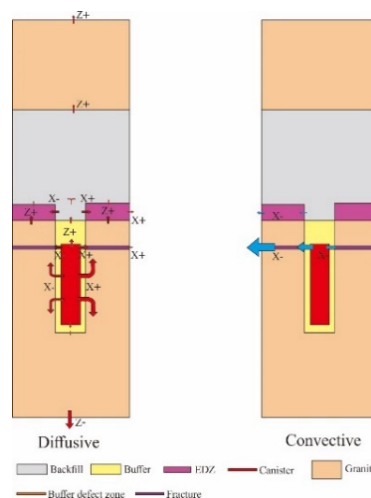


Figure 13. The transport mode of the modelling

Table 3. The total radionuclide transport at different boundaries of different domains

Boundary	Convective	Diffusive	Total
EDZ in X+ direction	0	-31.284	-31.284
EDZ in X- direction	-108.142	0	-108.142
Fracture in X+ direction	0	-2.827	-2.827
Fracture in X- direction	-8782.997	0	-8782.997
DEPOSIT in X+ direction	72.913	-160.517	-87.604
DEPOSIT in X- direction	-7740.163	-101.433	-7841.596
DEPOSIT in Y+ direction	-188.534	-342.173	-530.707
DEPOSIT in Y- direction	-188.535	-342.173	-530.708
DEPOSIT in Z+ direction	0.0003	-14.187	-14.1867
DEPOSIT in Z- direction	-0.001	-37.413	-37.414
Canister in X+ direction	1171.977	-1254.009	-82.032
Canister in X- direction	-6254.932	-137.856	-6392.788
Canister in Y+ direction	-359.882	-847.607	-1207.489
Canister in Y- direction	-359.882	-847.607	-1207.489
Canister in Z+ direction	-0.013	-104.067	-104.08
Canister in Z- direction	-0.001	-38.538	-38.538
TOTDOMAINE in X+ direction	0	-34.111	-34.111
TOTDOMAINE in X- direction	-8891.139	0	-8891.139
TOTDOMAINE in Z+ direction	0	-3.736	-3.736
TOTDOMAINE in Z- direction	0	-114.576	-114.576

5. Conclusion

This work of Scenario 1 demonstrates the sensitivity of the EDZ zone to the deposit hole. Only the gradient in horizontal direction was considered in this case. These results clearly indicate that the influence of the EDZ zone is enormous. The convective transport mass is bigger than the diffusive transport mass, which is about three times. The total transport mass through EDZ zone is about 91% of the source influx. The transport mass which across the granite boundary is very little. Moreover, the total flux out mass in Z+ direction is about 1/8 in Z- direction. Furthermore, both of the values are very small.

This work of scenario 2 mainly demonstrates the sensitivity of the fracture zone to the deposit hole. The size of the fracture aperture is 1000 mm, which is a bad fracture, actually. According to the geological survey data, the deep fracture is usually very small. In this case, it only considered the horizontal direction gradient. These results clearly indicate that the influence of the fracture zone is enormous. The convective transport mass is far more than the diffusive transport mass, which is about 55 times. Moreover, the leading path of convective is the fracture zone. The total convective transport mass which across the fracture zone is about 81 times of the EDZ zone. The transport mass which crosses the granite boundary is very little. Therefore, the deposits should prevent large fractures from the influence of the convective.

By assuming the safety cases in the single deposit scale at granite area, it is clearly to know the sensitivity of the fracture zone to the deposit hole. These results clearly indicate that the influence of the fracture zone is enormous. The convective transport mass is far more than the diffusive transport

mass. Moreover, the leading path of convective is the fracture zone. The transport mass which across the granite boundary is very little.

Acknowledgements

This work is a part of China-France associated laboratory of geological disposal. The main purpose of this work is to enhance the technical cooperation between China and France in the field of high-level radioactive waste disposal and to share the experience with each other in this field. In addition, this work has been supported by the Special Project on Decommissioning of Nuclear Facilities and Treatment of Radioactive Waste under grant number [2017] 1405.

References

- [1] Ales^ˇ V., Jir^ˇı L., Anton^ın V., Dus^ˇan V. (2015) A sensitivity and probability analysis of the safety of deep geological repositories situated in crystalline rock. *J Radioanal Nucl Chem.*, 304: 409–415.
- [2] Campbell, J.E., Cranwell, R.M. (1988) Performance assessment of radioactive waste repositories. *Science*, 239: 1389–1392.
- [3] DOE (US Department of Energy). (2008) Yucca Mountain Repository License Application, Safety Analysis Report. DOE/RW-0573. Office of Civilian Radioactive Waste Management, US Department of Energy, Washington, DC.
- [4] IAEA&NEA, (2006) Geological disposal of radioactive waste, Safety requirements. WS-R-4, Vienna.
- [5] Kim J.W., Cho D.K., Jeong J. (2014) A methodology for a risk-based approach to complex scenarios in a long-term safety assessment of a radioactive waste repository. *Nuclear Engineering and Design*, 268: 58–63.
- [6] Ling H. (2018) Postclosure Safety Assessment for High-level Radioactive Waste Repository in Beishan, China. BRIUG, Beijing.
- [7] PosivaOy. (2012) Safety case for the disposal of spent nuclear fuel at Olkiluoto-performance assessment 2012. POSIVA 2012-04. Eurajoki, Finland: Posiva Oy.
- [8] PosivaOy. (2012) Safety case for the disposal of spent nuclear fuel at Olkiluoto - synthesis 2012. POSIVA 2012-12. Eurajoki, Finland: Posiva Oy.
- [9] SKB(Svensk Kärnbränslehantering AB). (2006) Long-term safety for KBS-3 repositories at Forsmark and Laxemar-a first evaluation. SKB TR-06-09. Swedish Nuclear Fuel and Waste Management Co., Stockholm, Sweden.
- [10] SKB(Svensk Kärnbränslehantering AB). (2009) Groundwater flow modelling of period with temperate climate conditions-Forsmark. SKB R-09-20. Swedish Nuclear Fuel and Waste Management Co., Stockholm, Sweden.
- [11] SKB (Svensk Kärnbränslehantering AB). (2011) Long-Term Safety for the Final Repository for Spent Nuclear Fuel at Forsmark: Main Report of the SR-Site Project. SKB TR-11-01. Swedish Nuclear Fuel and Waste Management Co., Stockholm, Sweden.
- [12] SNL (Sandia National Laboratories). (2008) Total System Performance Assessment Model/Analysis for the License Application (Section 6). MDL-WIS-PA-000005. Sandia National Laboratories, Las Vegas, NV.
- [13] Witherspoon P.A., Bodvarsson G.S. (2001) In: Geological challenges in radioactive waste isolation: Third worldwide review. California. pp.77–84.
- [14] Wang J. (2010) High-level radioactive waste disposal in China: update 2010. *Journal of Rock Mechanics and Geotechnical Engineering*, 2: 1–11.
- [15] Wang J., Chen L., Su R., Zhao XG. (2018) The Beishan underground research laboratory for geological disposal of high-level radioactive waste in China: Planning, site selection, site characterization and in situ tests. *Journal of Rock Mechanics and Geotechnical Engineering*, 10: 411–435.